Optimal lockdowns: Analysing the efficiency of sanitary policies in Europe during the first wave

Ewen Gallic
Michel Lubrano
Pierre Michel

Optimal lockdowns: Analysing the efficiency of sanitary policies in Europe during the first wave[*]

Ewen Gallic[†]and Michel Lubrano[‡]and Pierre Michel[§]

February 18, 2021

Abstract

Uprising in China, the global COVID-19 epidemic soon started to spread out in Europe. As no medical treatment was available, it became urgent to design optimal non-pharmaceutical policies. With the help of a SIR model, we contrast two policies, one based on herd immunity (adopted by Sweden and the Netherlands), the other based on ICU capacity shortage. Both policies led to the danger of a second wave. Policy efficiency corresponds to the absence or limitation of a second wave. The aim of the paper is to measure the efficiency of these policies using statistical models and data. As a measure of efficiency, we propose the ratio of the size of two observed waves using a double sigmoid model coming from the biological growth literature. The Oxford data set provides a policy severity index together with observed number of cases and deaths. This severity index is used to illustrate the key features of national policies for ten European countries and to help for statistical inference. We estimate basic reproduction numbers, identify key moments of the epidemic and provide an instrument for comparing the two reported waves between January and October 2020. We reached the following conclusions. With a soft but long lasting policy, Sweden managed to master the first wave for cases thanks to a low $\mathcal{R}_0$, but at the cost of a large number of deaths compared to other Nordic countries and Denmark is taken as an example. We predict the failure of herd immunity policy for the Netherlands. We could not identify a clear sanitary policy for large European countries. What we observed was a lack of control for observed cases, but not for deaths.

Keywords: SIR models, phenomenological models, double sigmoid models, sanitary policies, herd immunity, ICU capacity constraint.
JEL codes: C22, C54, I18

[†]Aix Marseille Univ, CNRS, AMSE, Marseille, France
[‡]School of Economics, Jiangxi University of Finance and Economics, China and Aix Marseille Univ, CNRS, AMSE, Marseille, France
[§]Aix Marseille Univ, CNRS, AMSE, Marseille, France

1 Introduction

When the Coronavirus started to spread in Europe, the severity of the situation in Wuhan was already known. Because the virus was new and no treatment available, confinement and social distancing (non-pharmaceutical tools) were the only available solutions to slow down the epidemic. As this type of public policy can be extremely costly, decision makers urged epidemiologists to design various scenarios to predict the time when the epidemic would stabilize. The objective was to adjust public sanitary policies so as to minimize the time required for the resumption of economic activity and to smooth as much as possible the deleterious impact of the epidemic on growth.

Following these recommendations, all the European countries have adopted more or less stringent sanitary policies, having in mind either obtaining *natural herd immunity* or a temporary limitation of the number of cases to cope with Intensive Care Units (ICU) capacity with the hope to find a vaccine and finally gaining *artificial herd immunity*. In fact, there was no single policy, but a vast hesitation between different solutions, probably because of a mix between doubts about the results of the simulation models used by the epidemiologists and political or ideological constraints.

The epidemiological models, the most famous and simple one being the SIR model, divide the population into compartments, three for the SIR model, starting with Susceptibles (approximately the entire population), Infected (those who contract the virus) and Recovered who are those who, being once infected are either becoming immunized or die. The SIR model describes the transition between these three states, which corresponds to the evolution of the epidemic. The fundamental mechanism behind all these models is *herd immunity*. Once a sufficient number of people have been infected and thus immunized, the epidemic slows down and finally stops. Introducing the possibility of a lock-down in this model strongly modifies the basic reproduction number (the average number of people that one infected individual can contaminate when the virus is active in her body) and consequently the dynamics of the epidemic. The knowledge of these notions is of prime importance for governments in charge of sanitary policies to understand the mechanics of epidemics and to design non-pharmaceutical interventions (see, *e.g.*, Ferguson et al. 2020).

Two European countries have tried to rely on natural herd immunity to design their sanitary policies: Sweden and the Netherlands.[1] The other European countries have implemented much severe lockdowns, with the objective to slow down the epidemic to avoid congestion in ICU. In this context,

---

[1]For the Netherlands, see, *e.g.*, the article of Anna Holligan (4 April 2020) on BBC News: Coronavirus: Why Dutch lockdown may be a high-risk strategy. For Sweden, see, *e.g.*, the article of Maddy Savage (23 July 2020) Did Sweden's coronavirus strategy succeed or fail? on BBC News.

what is the best policy and is it possible to define what is an optimal policy? The objective of this paper is to try to answer this question by analysing both observed epidemiologic data and policy data by means of statistical models and confronting these results to the theoretical functioning of a SIR model. As polar cases, we shall considerer on one side Sweden and the Netherlands where policies were designed on the results of SIR models and on the other side the diversity represented by other European countries.

The interest in this question is amplified by the fact that the accuracy of the epidemiologic models was highly questioned in the academic press (see, *e.g.*, Begley, 2020, Adam, 2020, Jewell et al., 2020, Chin et al., 2020, among others). Despite their drawbacks, these models are the sole tools that we have to analyse counterfactuals such as *what would happen if nothing were done* and to establish and compare sanitary scenarios. In order to analyse the efficiency of the adopted sanitary policies, we have to model their consequences in term of cases, and deaths. For this, we rely on observed data and on statistical models. A class of useful models is known as phenomenological models or sigmoid models which come from biological growth theory. They are however closely related to SIR models as explained in Wang et al. (2012). These phenomenological models are thus the useful bridge between theory and data. Their statistical properties were thoroughly investigated in Ma (2020). We propose to use double sigmoid models (see, *e.g.*, Lipovetsky, 2010) to model the possible appearance of a second wave, which is the main risk attached to an inefficient sanitary policy. Equipped with this class of models, we can provide statistical inference for the basic reproduction number, establish comparisons between countries and finally analyse the impact of sanitary policies. For this purpose, we use the data set provided by the University of Oxford and the Blavatnik School of Government as it collects data on lock-down policies for 182 countries (as of December 9, 2020) and proposes a government severity index (Hale et al., 2020) together with the usual epidemic variables (confirmed cases and deaths).

The paper is organized as follows. In section 2, we show how to introduce lockdowns in a calibrated SIR model and how to characterize an optimal lockdown in two cases: when the objective is to get *natural herd immunity* or when the objective is to monitor ICU capacity. This is obtained by defining two alternative loss functions and minimizing these in a calibrated SIR model. In section 3, we present two statistical growth models, Richards and Gompertz, and define the key moments of an epidemic in this context. We then introduce double sigmoid models and define a policy efficiency index which compares the predicted size of two waves. In section 4, we describe the Oxford data set and the Wuhan survey which serves to calibrate a model for the mean serial interval. We justify the choice of ten European countries and present statistical inference for the basic reproduction number $\mathcal{R}_0$. For these countries, we compare the outbreaks of the first and second waves and draw some first conclusions. Section 5 is devoted to the analysing of

two unconventional sanitary policies (Sweden and the Netherlands). We compare their results first to the opposed case of Denmark and then to the diversity of large European countries. Section 6 concludes and discusses our main findings.

2 Optimal policies within a simulated SIR model

The SIR model of Kermack and McKendrick (1927) considers a finite and fixed population N which is divided into three exclusive groups (or compartments) summing to N: susceptibles S, infected I and removed R, these three letters giving its name to the model. A system of three differential equations describes the transitions between compartments. The strength of the epidemic or the infection rate β determines the transition from S to I. The recovery rate γ determines the passage from I to R. When an infected person recovers, she becomes immune to the disease and cannot be reinfected. A fourth equation can be added which predicts the number of deaths D within the removed, with death rate π. When normalizing the population to 1 so that $S + I + R = 1$, the system is completely described by the following differential equations:

$$\frac{dS}{dt} = -\beta I \times S, \tag{1}$$

$$\frac{dI}{dt} = \beta I \times S - \gamma I, \tag{2}$$

$$\frac{dR}{dt} = \gamma I, \tag{3}$$

$$\frac{dD}{dt} = \pi R. \tag{4}$$

Parameter γ is fundamentally a biological parameter which measures the rate of recovery when being infected. It is equal to the inverse of the number of days T_r needed to recover, $\gamma = 1/T_r$. With the COVID-19 pandemic, the average number of days to recover in most non-severe cases is between 7 to 14 days (see, *e.g.*, Park et al., 2020). This parameter is most of the time taken as fixed in applied work, with values ranging from $\gamma = 1/7$ (Moll, 2020) to $\gamma = 1/18$ (Wang et al., 2020). A middle range choice of $\gamma = 0.1$ was adopted in Toda (2020).

The second parameter, β is related to the contagiousness of the disease. It takes into account the probability of contracting the disease when a susceptible person comes into contact with an infected one. $T_c = 1/\beta$ can be thought as the typical time between contacts. The contact rate β is thus fundamentally a social parameter, because it depends on the habits of the population (shaking hands, wearing masks, population density...). It can vary a lot between countries and is the main object of inference when these

models, in their probabilistic formulation, are confronted to count data (see, *e.g.*, Clancy and O'Neill, 2008, Ma, 2020, Toda, 2020).

The last parameter π is the probability of dying when infected. Most of the controversies reported in the literature (see for instance Adam, 2020) concern the predicted number of deaths. The fatality rate π is very hard to estimate because cases are under-reported by lack of tests at the outbreak of the epidemic while the number of deaths are reported more accurately. By early December 2020, the empirical fatality rate varied between 0.9% (Denmark) to 3.5% (UK and Italy). The value adopted in Ferguson et al. (2020) was 0.9%, a value taken for instance in Roques et al. (2020) for France.

Typical initial conditions are:

$$S_0 = 1 - I_0, \qquad I_0 \simeq 0, \qquad R_0 = 0,$$

implying that we have to choose I_0. The usual, but unsatisfactory, solution is to fix $I_0 = 1/N$. It is better to select I_0 so as to obtain a particular date for the peak of the epidemic or a given value for I_t at a particular date t, given the other parameters.

2.1 Reproduction numbers

The basic reproduction number $\mathcal{R}_0$, *i.e.*, the average number of persons that an infected person manages to contaminate during the period of contagion is given by $T_r/T_c = \beta/\gamma$. This number is fixed at the beginning of the epidemic and constitutes its main characteristics. For COVID-19, the first values taken in the model initiated by Neil Ferguson at Imperial College (see Ferguson et al., 2020) were between 2 and 2.6, later updated to an interval between 2.4 and 3.3 for the United Kingdom. In European countries, values as high as between 3.0 to 4.7 were found as reported in Adam (2020). We estimated values ranging from 1.81 (Sweden) to 3.79 (Italy).

The effective reproduction number $\mathcal{R}_t^e$ characterizes the evolution of the epidemic over time:

$$\mathcal{R}_t^e = \frac{\beta}{\gamma} \times S_t = \mathcal{R}_0 \times S_t.$$

It decreases with the proportion of susceptibles S_t. If $\beta > \gamma$ (implying $\mathcal{R}_0 > 1$), the epidemic grows exponentially. If $\beta < \gamma$ (implying $\mathcal{R}_0 < 1$) it dies out exponentially.

The model assumes that an infected person recovers (or dies), but can never be re-infected. Because of the conservation identity $S + I + R = 1$, the number of susceptibles decreases while the number of recovered increases. But if in the long run I tends to 0, the number of susceptibles does not decrease to zero, because of herd immunity. Herd immunity is reached when a sufficient proportion of individuals have been infected and have become

immune to the virus. This proportion R^* of immune people depends on the contagiousness of the disease:

$$R^* = 1 - 1/\mathcal{R}_0.$$

It is in direct relation to the number of death with (4). To R^* corresponds the equilibrium proportion of remaining people in the susceptible group:

$$S^* = 1/\mathcal{R}_0.$$

This proportion is reached at the peak of the epidemic and is usually lower than the limiting value S_∞ when $t \to \infty$. So the model is overshooting over S^* by a non-negligible percentage. With a plausible value of $\mathcal{R}_0 = 2.5$ for the COVID-19, the herd immunity threshold is $S^* = 0.4$, meaning that herd immunity is reached when $R^* = 0.60$, i.e 60% of the population has been removed. The percentage of overshooting can be calculated directly from the equilibrium solution of the model. Combining the two equations (1)-(3) defining S and R, integrating from 0 to t and using the conservation identity, we get:

$$I_t = 1 - R_0 - S_t + \frac{1}{\mathcal{R}_0} \log \left(S_t/S_0 \right). \tag{5}$$

When $t \to \infty$, the number of infected become zero ($I_\infty = 0$). If $R_0 = 0$, it comes that the equilibrium is given by:

$$S_t = 1 + \frac{1}{\mathcal{R}_0} \log(S_t/S_0).$$

For $\mathcal{R}_0 = 2.5$ and $I_0 = 10^{-4}$, $S_\infty = 0.107$. So that the model overshoots the number of cases by $S^* - S_\infty = 0.4 - 0.107 = 0.293$.[2]

2.2 Dynamics and phase diagrams

The dynamics of a model is best described using a phase diagram (see, *e.g.*, Vespignani 2011). For a SIR model (Rachel 2020), it consists in plotting S against I, assuming $S + I \leq 1$. To obtain this graph, the system of differential equations representing the core of the SIR model has to be solved. Euler's method is straightforward to apply with:
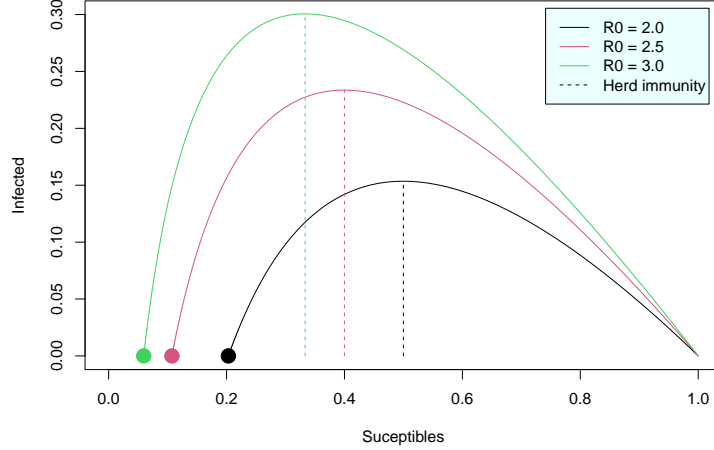
$$
\begin{align}
S_i &= S_{i-1} - \beta S_{i-1} I_{i-1} \Delta t, \tag{6}\\
I_i &= I_{i-1} + (\beta S_{i-1} I_{i-1} - \gamma I_{i-1}) \Delta t, \tag{7}\\
R_i &= I_{i-1} + \gamma I_{i-1} \Delta t, \tag{8}
\end{align}
$$

where $\Delta t < 1$ is the discretization step. Figure 1 shows the trajectory of the

---

[2]The equilibrium equation can be solved using Brent's algorithm (Brent, 1973) in order to find S_∞.

The vertical dashed lines represent both the peak of the epidemic and the level of herd immunity. The dots indicate the end of the epidemic and the remaining proportion of suceptibles.

Figure 1: Over shooting after herd immunity visualized in a phase diagram

epidemic for various $\mathcal{R}_0$. Herd immunity is given by $S^* = 1/\mathcal{R}_0$, the point at which the number of infected persons starts to decrease, S^* corresponding to the peak of the epidemic. The epidemic stops at a much lower proportion of susceptibles which is indicated by a big dot on the graph. With a phase diagram, we can visualize the gap existing between herd immunity S^* and the final proportion of suceptibles S_∞.

The aim of a sanitary policy is to reduce this gap to zero, by this way limiting the number of deaths. In the absence of any policy intervention, the predicted total number of deaths D_N is given by:

$$D_N = (1 - S_\infty)\,\pi \times N \times S_0. \tag{9}$$

The first term indicates the proportion of recovered when at the end of the epidemic $I_\infty = 0$ and $N \times S_0$ represents the population which is concerned by the epidemic (after removing those already immunized $(1 - S_0)$ before the start of the epidemic). With a death rate equal to $\pi = 0.009$ (as assumed in the Imperial College model) and a population of $N = 66$ millions for France or the United Kingdom, the total number of deaths would be around 538 000, a figure which is of the same order of magnitude to that reported by Imperial College in March 2020 (see, *e.g.*, Adam, 2020). With an optimal sanitary policy achieving $S_\infty = S^*$, this number would be reduced to:

$$D_N = (1 - S^*)\,\pi \times N \times S_0. \tag{10}$$

360 000 in our case. These figures are of course conditional on the hypothesis

and limitations of the model, in particular homogeneity of the population. This explains why they are at odds with the real figures of France and the United Kingdom which were respectively 30 000 and 45 000 on July 12, six month after the start of the pandemic.

2.3 Lockdowns in a SIR model

If the aim of a sanitary policy is easy to define (limiting the number of deaths), it becomes difficult to design it precisely. Rachel (2020) among others has proposed a theoretical model which shows that the optimal policy implements social distancing and is almost independent of economic parameters (value of life, functioning of the labour market). So the simple SIR model can be taken as a benchmark.

A lock-down is introduced in the SIR model by considering a time variable β_t. If ℓ_t is the strength of the lock-down and β_0 the value of β in the absence of a lock-down, then:

$$\beta_t = \beta_0 \times (1 - \ell_t),$$

It implies that the effective reproduction number is reduced to:

$$\mathcal{R}_t^e = (1 - \ell_t)\mathcal{R}_0 S_t.$$

With a very strict lock-down the epidemic stops to spread out. But that does not mean that the epidemic will cease, once the lock-down is removed. So let us define next what is an optimal lockdown.

2.4 Optimal lockdowns based on herd immunity

For designing a lock-down, three parameters are at work: starting date θ_t, length θ_l, and severity θ_s and $\theta' = (\theta_t, \theta_l, \theta_s)$. In order to find the three parameter values of an optimal policy, we simulate the calibrated model (1)-(3) solved using Euler's discretization so as to minimize the following quadratic loss function:

$$loss = (S_\infty(\theta) - 1/\mathcal{R}_0)^2 + (I_\infty(\theta)) - I_0)^2. \qquad (11)$$

This function means that at a point $t^* = \theta_t < T$ (T being the length of the simulation period), we have reached $S_t^* = S^*$ and that the number of new infected I_t^* has returned to its initial value. The objective of this loss function is to reach herd immunity, without any concerned on the maximum number of infected.

Let us choose three different values for $\mathcal{R}_0$: 2.0, 2.5 and 3.0. For γ, we adopt the standard value of 0.10. The model is solved with a discretisation step of $\Delta t = 0.01$ and prediction horizon of $T = 300$. The peak is obtained when $I(t)$ reaches its maximum. The acceleration of the epidemic

corresponds to the point in time when $\Delta I(t)$ reaches it maximum. In order to make things comparable between the three cases, we have chosen the initial condition I_0 so that the peak of the epidemic in the absence of any intervention is located at $t = 65$. The characteristics of the simulation are

Table 1: Characteristics of the calibration

$\mathcal{R}_0$	I_0	S^*	S_∞	Accel.	Peak	Decel.	End	D_∞	Max I_t
2.0	$1.24\ 10^{-3}$	0.50	0.203	49	65	82	207	480	0.154
2.5	$9.39\ 10^{-5}$	0.40	0.107	53	65	77	185	538	0.234
3.0	$4.54\ 10^{-6}$	0.33	0.060	56	65	75	211	567	0.301

Calibration of I_0 so as to get a peak at $t = 65$ was done using Brent algorithm with starting interval [0-0.05] for $\mathcal{R}_0 \leq 2.0$ and [0-0.01] for $\mathcal{R}_0 > 2.0$. The end of the epidemic is defined as $I_t \leq I_0$ for $t > t_{peak}$. The number of deaths is indicated in thousands for a reference population of 66 millions.

summarized in Table 1. The corresponding phase diagrams are given in Figure 1.

Given these initial conditions, the minimization of loss function (11) provides the optimal design of a lockdown reported in Table 2. We find

Table 2: An optimal lockdown policy

$\mathcal{R}_0$	Start	Severity	Length	End	Death	Max I_t
2.0	60	0.65	84	143	305	0.144
2.5	60	0.68	81	141	368	0.212
3.0	61	0.73	78	139	409	0.272

The loss function was minimized using the derivative free method of Nelder-Mead in `optim` of R. Starting values are start=55, severity=0.70 and length=80. The number of deaths is indicated in thousands for a reference population of 66 millions.

that we have to wait between 1 and 4 days before the peak and then we should impose a rather severe lockdown lasting at least 78 days. Under those conditions, herd immunity will be reached during the lockdown. And the lockdown will end between 46 and 72 days before the computed end of the epidemic ($I_t < I_0$) in the absence of any intervention. If the lockdown manages to reduce to reduce the number of deaths, it has only a mild impact on the maximum percentage of infected. So this type of lockdown is not adapted when there is a ICU capacity limit, except when $\mathcal{R}_0$ is very low. This is the reason why we shall qualify this policy as *unconventional*.

This optimal lockdown might be difficult to implement, because its starts very late and is rather strong. So a political variable can be the date when to start. In this case, we fix the starting date well before the peak and minimize the loss function (11) with respect to only two parameters, severity and length. Results are regrouped in Table 3 for $\mathcal{R}_0 = 2.5$.

Because the acceleration point is at $t = 53$, it is not efficient to start too

Table 3: $\mathcal{R}_0 = 2.5$

Start	Severity	length	End	R^*	R_∞	Deaths	Max I_t
45.00	0.42	141	186	0.60	0.61	373	0.089
50.00	0.46	137	187	0.60	0.61	369	0.115
55.00	0.53	133	188	0.60	0.60	364	0.172
60.00	0.69	114	174	0.60	0.60	363	0.218

The loss function was minimized using the derivative free method of Nelder-Mead in `optim` of R. Starting values are severity=0.70 and length=80. End is the end of the lockdown. The number of deaths is indicated in thousands for a reference population of 66 millions.

early at $t = 45$ or at $t = 50$. At the end of the confinement, the optimal R^* is reached, but after the release of the confinement, there is a small rebound. The advantage of starting 10 days before the peak is that the severity of the lockdown is lower, but at the cost of an increased length. There is no additional cost is term of deaths.
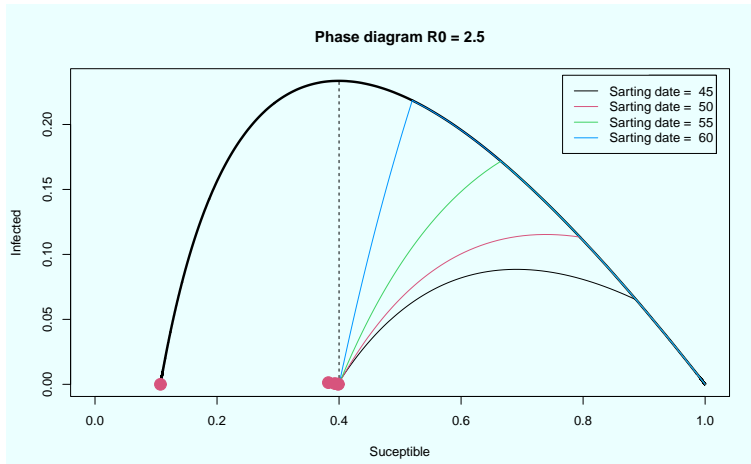
Lockdown severity is indicated in the box for starting dates corresponding to $t = 45$, $t = 50$, $t = 55$, $t = 60$ and $t = 63$. Herd immunity corresponds to the dashed vertical line. The black thick line corresponds to the original trajectory of the epidemic.

Figure 2: Phase diagram of optimal lockdown policies with different starting dates

Figure 2 show the different trajectories to reach S_*, and the trade-off between an early starting date and lockdown severity.

A lockdown becomes inefficient if too strong or started too early. We consider three possible starting dates, $t = 40$, $t = 45$ and $t = 50$, before the peak ($t = 65$) and the acceleration date ($t = 53$). The severity index is chosen to be 0.88 and the length 55 days, values corresponding to the lockdown implemented in France in March 2020 (see Table 7). As seen in Figure 3, a second wave is appearing quite soon after the end of the

lockdown, just because a tight lockdown prevented herd immunity to be reached.
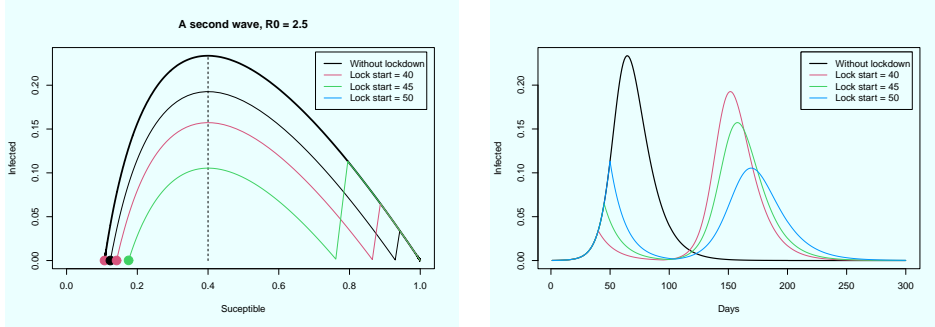

Figure 3: A second wave due to a failing lockdown

In the SIR model, a successful lockdown reaches herd immunity, while avoiding a second wave. As a matter of fact, the three simulated lockdowns led to a proportion of people affected by the epidemic R_∞ of 0.88, 0.86 and 0.83 (with starting dates of respectively 40, 45 and 50) instead of the optimum of $R^* = 0.60$. So the appearance of a second wave entails that the final number of deaths is much higher if a second lockdown is not implemented.

2.5 Optimal lockdown with ICU constraint

An alternative policy is to focus on hospital capacity (see, *e.g.*, Pathak et al. 2020). It is defined as a percentage ξ to be compared to the maximum proportion of infected people over the period, leading the following alternative loss function:

$$loss = 100 \times (\max_t(I_t(\theta) - \xi)^2 + (I_\infty(\theta) - I_0)^2.$$

It includes the previous objective of no infection at the end of the simulation period, but put a strong weight on ICU capacity constraint. We have chosen $\xi = 0.05$ as in Pathak et al. (2020).

The chosen confinement profile is also different. It is equal to 0.0 before the starting date, then goes up to θ_s for a period equal to θ_t which are the two parameters to be found by optimization as in the previous case. But instead of returning to zero, there is a follow up period with mild conservatory sanitary measures of severity parameter that we fixed equal to 0.25 and which lasts till the end of the simulation horizon $T = 300$.

The obtained optimal policy is totally different as reported in Table 4 with phase diagram and epidemic trajectories given in Figure 4. This alternative policy is characterized by a very long confinement of 169 days, the double of what was required to get herd immunity in Table 2. But the severity is rather mild (0.43 compared to 0.68 in Table 2), provided that

11

Table 4: A very long lockdown waiting for a vaccine

Start	Severity	Length	R_T	Deaths
20	0.43	169	0.46	358
30	0.44	107	0.38	390
40	0.48	64	0.31	401

Start is the starting date in days since the beginning of the epidemic. R_T is the proportion of removed at the end of the simulation horizon $T = 300$. With a $\mathcal{R}_0 = 2.5$, $R^* = 0.40$. The number of deaths is indicated in thousands for a reference population of 66 millions.
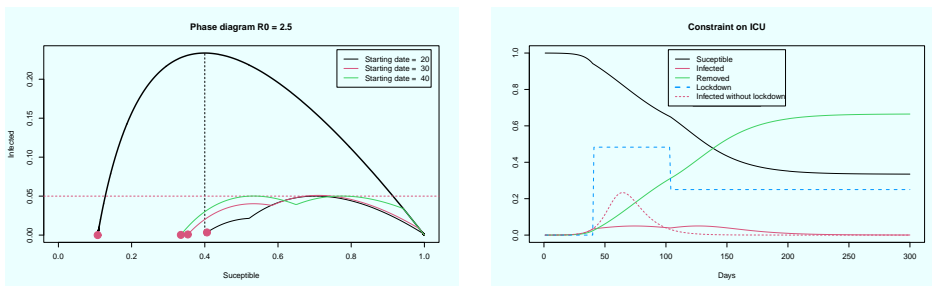

Figure 4: Waiting for a vaccine with a very long confinement

the confinement is followed by permanent but mild conservatory sanitary measures (0.25). It is optimal to start the confinement 20 days after the very start of the epidemic, so much earlier than what indicated in Table 2. As a matter of fact, after 20 days, the simulated infection rate is 0.0019, well below $\xi = 0.05$. With this policy, the final number of death is strictly equivalent to that obtained with the unconventional policy of Table 2 based on reaching herd immunity.

We have to define what is a policy failure in this case. Obviously, the existence of a second wave is not sufficient. When the lockdown starts early enough, the second wave does not lead to an overshooting, as shown in Figure 4 so that at the end it has no incidence on the total number of deaths which remains the same as in the case of a successful policy based on herd immunity. Here again success occurs when $S_\infty = S^*$. In Figure 4, the second wave is much below the first one. And the larger the second wave, the larger the overshooting. So even if suppressing the overshooting is no longer included in the loss function, its absence can be used as a measure of success.

3 Phenomenological models for modelling waves

Epidemiologic models are convenient for designing policies, but they are difficult to fit to actual data because of their built-in constraints. Instead of introducing heterogeneity in the population (age groups) as in Pathak et al.

(2020) or Acemoglu et al. (2020), we prefer to consider more simple statistical models coming from the biological literature on growth of species (see Turner et al., 1976, Tsoularis and Wallace, 2002 or Ma, 2020 for a survey). Moreover, as explained in Wang et al. (2012), they can encompass the main features of a SIR model.

3.1   Richards and Gompertz models

For analysing the similarity between the SIR model and population models, Wang et al. (2012) consider the following growth equation for confirmed cases $C(t)$:

$$\frac{dC}{dt} = rC \left[1 - \left(\frac{C}{K} \right)^{\delta} \right], \tag{12}$$

with r, δ and K being positive real numbers. This equation covers two mechanisms. A growth rate with the term rC that corresponds to the epidemic at its beginning, equivalent to an exponential model. A reversion mechanism (or self-regulating) with the term $\left[1 - (C/K)^{\delta} \right]$ which says that the epidemic C will anyway reach a maximum K. Note that in this model the maximum K is estimated while the total number of susceptibles is fixed beforehand in the initial conditions of the SIR model. This growth equation corresponds to Richards' model (Richards 1959). More general generating equations are considered in Turner et al. (1976) or Tsoularis and Wallace (2002), but are not useful for our purpose.

The solution to equation (12) corresponds to:[3]

$$C(t) = \frac{K}{\left[1 + \delta \exp\left(-r(t - \tau) \right) \right]^{1/\delta}}, \tag{13}$$

with the property that $\lim_{t \to \infty} C(t) = K$. This parameterization introduces a new parameter τ which monitors the date of occurrence of the peak ($t = \tau$) with value:

$$C_{inf} = \frac{K}{(1 + \delta)^{1/\delta}}.$$

So $\delta > 0$ monitors the value of the curve at the inflection point and the asymmetry around $t = \tau$. This point is of particular importance because it corresponds to the period when the epidemic starts to regress, or equivalently when the effective reproduction number R_t starts to be below 1 in a SIR model.

---

[3]Note that this writing is the usual model detailed in the literature, when the solution to the differential equation (12) is slightly different with $C(t) = K \left[1 + \delta \exp\left(-r\delta(t - \tau) \right) \right]^{-1/\delta}$, see Wang et al. (2012).

The first order derivative $C'(t)$ of this function provides an estimate of the number of cases at each point of time:

$$C'(t) = \frac{Kr \left[\delta \exp\left(r(\tau - t)\right) + 1\right]^{-1/\delta}}{\delta + \exp\left(r(t - \tau)\right)}.$$

The growth rate is equal to r/δ while the relative speed defined as $C'(t)/C(t)$ is given by:

$$\frac{C'(t)}{C(t)} = r \frac{e^{-r(t-\tau)}}{1 + \delta e^{-r(t-\tau)}}.$$

When imposing a restriction on δ in (13), we get two of the usual models of the literature. The logistic model (Verhulst 1845) is obtained for $\delta = 1$. Its inflexion point is $K/2$, just midway between the start and the end of the epidemic, a restriction which is unrealistic for the Covid-19. The model of Gompertz (Gompertz 1825) is obtained by taking the limit of (13) for $\delta \to 0$ which gives:[4]

$$C(t) = K \exp\left[-\exp\left(-r(t - \tau)\right)\right].$$

The corresponding inflexion point is:

$$C_{inf} = Ke^{-1}, \tag{15}$$

So Gomperz model is a very parsimonious way of obtaining an inflexion point lower than $K/2$. The first order derivative of this function provides an estimate of the number of cases at each point in time:

$$C'(t) = Kr \exp\left[r(\tau - t) - \exp\left(r(\tau - t)\right)\right].$$

So that the relative speed of the epidemic is given by:

$$\frac{C'(t)}{C(t)} = re^{-r(t-\tau)}.$$

3.2   Key moments of an epidemic wave

After the starting point t_S which usually appears with the first cases, the acceleration phase corresponds to the period of exponential growth of the epidemic. In a sigmoid model this period ends in t_A when the second order derivative reaches its maximum and when the exponential model used in

---

[4]In this case, the generic equation would be:

$$\frac{dC}{dt} = \lim_{\delta \to 0} \frac{r}{\delta} C \left[1 - \left(\frac{C}{K}\right)^{\delta}\right] = rC \log\left(\frac{K}{C}\right). \tag{14}$$

section 4.4 ceases to be relevant. The peak of the epidemic is reached later at t_P when the second order derivative is zero. This corresponds also to $t = \tau$ in the parameterization adopted above, the point where $C(t) = C_{inf}$. Then follows a phase of deceleration which is maximal at $t = t_D$ when the second order derivative reaches its minimum. This is not yet the end of the epidemic. Beyond this point, the number of new cases is still positive. It becomes zero for $t \to \infty$. Table 5 summarizes this information.

Table 5: Key moments of an epidemic wave as a function of $C(t)$.

Key moment	Description	Time point t
Acceleration	Beginning of the growth phase, maximum acceleration	$t_A = \underset{t>0}{\operatorname{argmax}}\, C''(t)$
Peak	Peak of the epidemics, null acceleration	$t_P = \arg_{t>t_A} C''(t) = 0$
Deceleration	End of growth phase, minimum acceleration	$t_D = \underset{t>t_P}{\operatorname{argmin}}\, C''(t)$

Figure 5 illustrates the sensitivity of the position of these key moments to the value of δ.

Figure 5: The position of key moments depends on δ
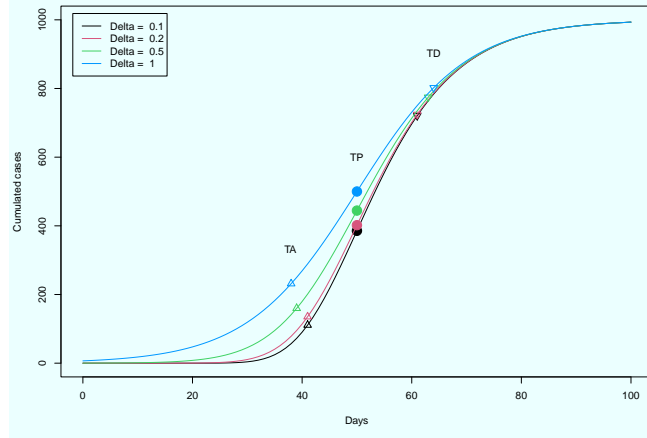
Note: The points t_A, t_P, and t_D represent respectively: acceleration, peak, deceleration.

The estimation of Richards' model on European data will have a tendency to favour rather low values of δ, so that in many occasions Gompertz' model will be the most parsimonious choice. Consequently, the acceleration point will be quite close to the peak and the later quite far away from the deceleration point. This implies that when the data are well described by a Gompertz model, we are far from being in a safe situation after the peak, rendering deconfinement a delicate procedure.

15

3.3 Double sigmoid functions to account for a second wave

An inadequate deconfinement (or an inefficient confinement) leads to the up-spring a significant second wave and an overshooting. The importance of this second wave provides a direct measurement of the efficiency of the sanitary policy decided during the first wave, whatever the type of policy chosen. In order to detect and measure the impact of this second wave, we need to add a second member to our initial phenomenological model, leading to what the literature called double sigmoid models, formalized as:

$$C(t) = C_1(t) + C_2(t), \tag{16}$$

where $C_1(t)$ is the first sigmoid function and $C_2(t)$ the second one. This type of model appeared quite early in the literature with Bock et al. (1973) or Thissen et al. (1976) and led to some developments with Lipovetsky (2010) or Oswald et al. (2012). If we consider two Gompertz curves, we have:

$$C(t) = K_1 \exp\left[-\exp\left(-r_1(t - \tau_1)\right)\right] + (K_2 - K_1) \exp\left[-\exp\left(-r_2(t - \tau_2)\right)\right].$$

K_1 and K_2 are the intermediate and final plateau of saturation so that $\lim_{t \to \infty} C(t) = K_2$. τ_1 and τ_2 monitor the position of the peak of each phase while the growth of the process is determined by r_1 and r_2. However there is no analytical formula to determine the value and position of the two peaks. We have to locate numerically the extremum of the first order derivative of $C(t)$:

$$\begin{aligned} C'(t) = &K_1 r_1 \exp\left[-r_1(t - \tau_1) - \exp\left(-r_1(t - \tau_1)\right)\right] + \\ &(K_2 - K_1)r_2 \exp\left[-r_2(t - \tau_2) - \exp\left(-r_2(t - \tau_2)\right)\right], \end{aligned}$$

As a by-product $C'(t)$ provides an estimate of the number of cases at each point of time.

3.4 Measuring policy efficiency

An efficient policy is difficult to design, because its parameters depend on the key moments of the trajectory of the epidemics in the absence of any intervention, which of course are not observed. But knowing $\mathcal{R}_0$, a calibrated SIR model could provide this information. What we observe is the impact of the confinement on the dynamics of the first wave, an information that help to estimate $C_1(t)$. With an unconventional fully efficient sanitary policy, the epidemic would stop after $C_1(t)$, no second wave would appear and the final size of the epidemic would be K_1. With an efficient sanitary policy based on ICU capacity, a mild second wave should appear. The final size of the epidemic would be K_2, but with $K_1 \simeq K_2$.

In most countries, a second wave has appeared after the end of July and so the second component $C_2(t)$ becomes necessary for modelling the complete time span. Comparing the strength of the two waves would provide a measure of efficiency of the first confinement. Extending $C_1(t)$ after the end of July would provide a counter factual for a tamed epidemic which has to be compared to the full observed spell measured by $C_1(t) + C_2(t)$.

Now let us discuss more precisely the content of $C_2(t)$. Because our research question is to measure the efficiency of the sanitary policy implement during the first wave, we have to end our sample before any new strong strong measure designed to fight the second wave. So either $C_2(t)$ has to be chosen among the exponential class of models (possibly the generalized exponential model) or we have to provide a prior information on the value of τ_2 as by definition the second peak will be outside our sample, creating an identification problem for τ_2. Once τ_2 is fixed and r_2 estimated, K_2 becomes identified. Consequently if $C_1(t)$ and $C_2(t)$ belong to the same family, conditionally on an upper limit for τ_2, a relative measure of inefficiency of the first confinement is provided by the distance between $C_1(t)$ and $C_1(t) + C_2(t)$, measured for instance by the ratio:

$$\frac{C_1(t)}{C_1(t) + C_2(t)}.$$

For $t \to \infty$, this ratio tends to K_1/K_2. It represents the loss in efficiency occurring because of the second wave.
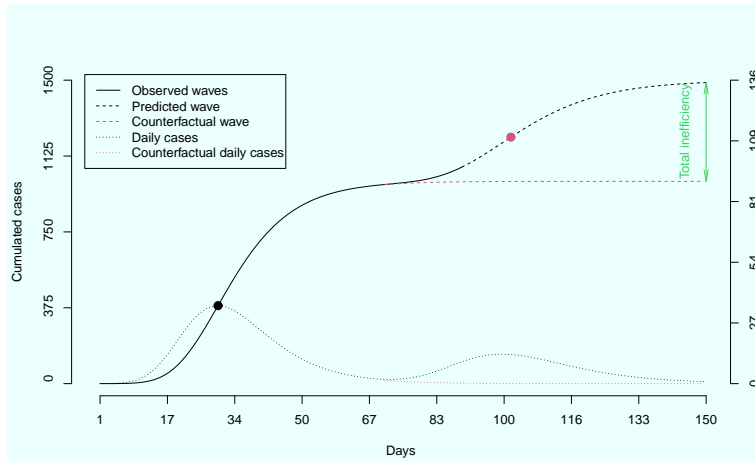
The green arrow measures total inefficiency for the predicted second wave. The black dot indicates the first peak and red dot the estimated second peak. The scale of daily observations is indicated on the right.

Figure 6: Measuring and predicting policy inefficiency

Figure 6 visualizes the two waves, both in daily values and in cumulated values. Total inefficiency is measured as the total number of supplementary

17

cases that are induced by the second wave. Relative inefficiency corresponds to the ratio K_1/K_2.

4   Data and first empirical results

The fact that COVID-19 was declared a pandemic by the World Health Organization (WHO) generated the production of several data bases that were essential for monitoring sanitary policies, the most well known being the COVID-19 Data Repository by the Center for Systems Science and Engineering (CSSE) at Johns Hopkins University (JHU CSSE COVID-19 Data).[5] However, this data base does not give any indication on the sanitary policies that were implemented in every country, at odds with the data set provided by the University of Oxford.

4.1   The Oxford data set

The University of Oxford and its Blavatnik School of Government collected data on lock-down policies for 182 countries and derived various government response indices which are helpful to appraise the severity of these policies (Hale et al., 2020). These indices are constructed from various ordinal measures of the severity of policies undertaken by governments. Each ordinal scale represents one aspect of the severity of closures and containment (school and workplace closures, cancelling public events, bans on private gatherings, closing of public transport, stay at home requirements, restrictions on internal movement), economic measures (income support, freezing financial obligations), or health measures (public information campaigns, testing policy, contact tracing). The three global indices vary between 0 and 100, 0 indicates a "*laissez-faire*" policy, and 100 indicates the highest level of severity of government response. Details on the composition of the indices are provided in Hale et al. (2020). Among those indices, we have chosen the Stringency Index which accounts for 9 items related to confinement and health information. The database provides also as complementary information, the usual count epidemic variables: confirmed cases and number of deaths.[6]

---

[5] Those data are described on JHU website (https://coronavirus.jhu.edu) and can be downloaded on a github repository (https://github.com/CSSEGISandData/COVID-19).

[6] The data base can be accessed at https://github.com/OxCGRT/covid-policy-tracker/raw/master/data/OxCGRT_latest.csv. JHU and Oxford are providing similar information for confirmed cases and deaths. For most countries there are only minor differences. However for France, the differences are huge because of different convention for taking into account some sources. The JHU series presents a large kink for April 12 and then is systematically higher than the Oxford series by 30%.

4.2 The Wuhan survey

Individual survey data are necessary to medically characterize the virus. Because the epidemic started in Wuhan, a Chinese team led a preliminary survey, collecting individual data in this city. It had its origin in the surveillance mechanism for pneumonia of unknown source, which started after the SARS outbreak in 2002. First cases of a new form of pneumonia were reported in Wuhan by early December 2019. The early survey based on field interviews by members of the Chinese Center for Disease Control (China CDC) yielded data on 425 confirmed cases in Wuhan between December 2019 and January 2020. Using this survey, Li et al. (2020) managed to determine the epidemiological characteristics of the Covid-19. First cases were identified in hospital by December 29, 2019. First dates of onset were around December 10, 2019. Realistic numbers of declared cases are available till January 8, 2020. The distribution of the *incubation period* was estimated by fitting a lognormal distribution on exposure histories, leading to an estimated mean of 5.2 days, a 95% confidence interval of [4.1,7.0] and the 95th percentile of 12.5 days.[7] The *mean serial interval* is defined as the time between the onset of symptoms in a primary case and the onset of symptoms in secondary cases. Li et al. (2020) fitted a gamma distribution to data from cluster investigations. They found a mean time of 7.5 days (sd = 3.4) with a 95% confidence interval of [5.3,19].[8] These pieces of information correspond to the general characteristics of the virus. For its propagation in Wuhan, they found that the number of cases doubles every 7.4 days in the early stage and that the basic reproduction number was estimated to be $\mathcal{R}_0 = 2.2$ with a 95% confidence interval of [1.4,3.9]. Subsequent articles report on average larger values of $\mathcal{R}_0$ ranging from to 1.9 to 6.47 and lower doubling times, ranging from 2.9 to 7.4 days (Park et al., 2020).

4.3 Choosing ten European countries

We focus our attention on ten European countries which are representative of the different phases of the pandemic and also of the different sanitary policies that were applied to contain national epidemics. For ease of presentation, these countries are divided in two groups according to their population: France, Germany, Italy, Spain, and the United Kingdom for large countries and Belgium, Denmark, Ireland, the Netherlands and Sweden for smaller countries.[9] All the samples begin on January 22, 2020, which is totaly suitable to describe the first wave and the first sanitary policies that were

---

[7]This corresponds to a lognormal density with parameters $\mu = 1.43$ and $\sigma = 0.67$.

[8]The corresponding parameters of the gamma distribution are 4.87 for the shape parameter and 1.54 for the scale parameter.

[9]The respective population of large countries is in millions: Germany 83, France 67, the UK 66, Italy 60, Spain 47. For smaller countries: the Netherlands 17, Belgium 11, Sweden 10, Denmark 6, Ireland 5.

implemented. We decided to stop our sample by the end of September 2020, sometimes going up to mid October, 2020 because our aim is to be able to characterize the beginning of the second wave and the success or failure of the various de-confinements, following the first wave. The precise stopping date is discussed in section 5.

Figure 7: Confirmed cases.
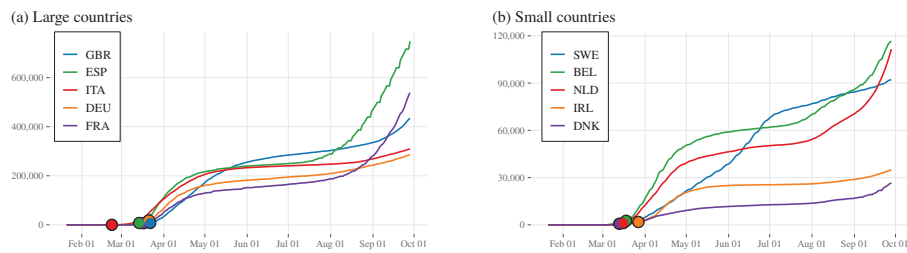
Note: The dots indicate the time when at which the government response index becomes greater than 60.
Source: University of Oxford, Blavatnik School of Government.

Graphs corresponding to confirmed cases for large and small countries are displayed in Figure 7. Italy was the first European country hit by the epidemic and reported the first confirmed cases around the beginning of March 2020. There has been a delay in both the onset of the epidemic and differences in the speed of propagation. Among larger countries, Italy was the first to start to impose a strict confinement and the United Kingdom the last one. The situation in smaller European countries was much more diverse. The epidemic started around the same time, but with totally different speeds with high speed for the Netherlands and Belgium and low speed for Sweden, Ireland and Denmark. Note the very peculiar evolution of cases for Sweden, providing thus an emblematic case study.
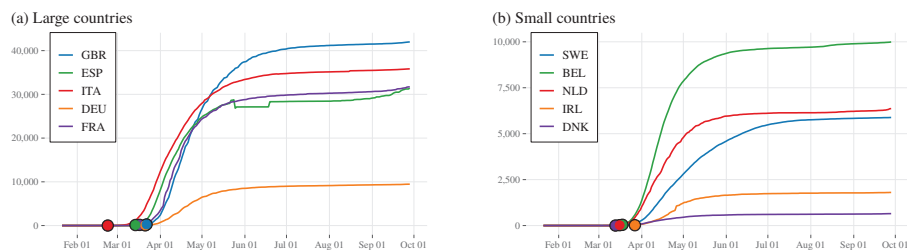
Figure 8: Confirmed deaths.

Note: The dots indicate the time when at which the government response index becomes greater than 60.
Source: University of Oxford, Blavatnik School of Government.

Figure 8 displays the cumulative evolution of the number of deaths. The

20

most striking fact is that the final ordering does not correspond to the confirmed cases ordering. The United Kingdom was the last to impose strict confinement which logically led to the greatest number of cases and deaths. But this apparent logic is not followed for the other large countries. France and Germany started to confine at roughly the same date. But the number of deaths in Germany was the third than that of France, perhaps due to a better public health system. For small countries, the lack of strict confinement could explain the linear increasing number of cases, but not the fact that both Belgium and the Netherlands had a larger number of deaths. There is thus a variety of situations because what we observe is the interplay between different sociological habits (different values of β in a SIR model) and a variety of sanitary policies with the intuition that none of them was fully optimal.

Figure 9: Government response index.
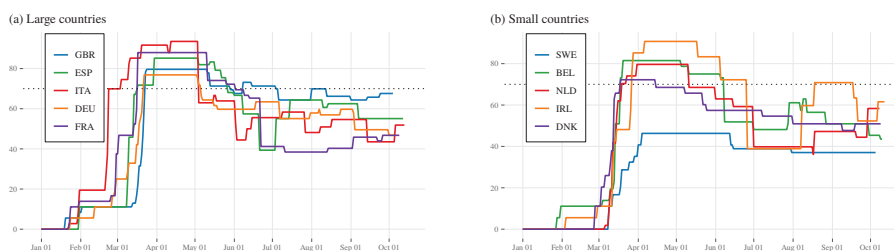
Note: the grey dotted horizontal highlights the level 70 for the government response index.
Source: University of Oxford, Blavatnik School of Government.

The stringency index reflects in Figure 9 the large diversity of non-pharmaceutical interventions in reaction to the outbreak of the epidemic in March and to the appearance of a second wave by the end of August. In Table 6, we try to characterize these differences in term of speed of reaction to the outbreak of the epidemic. The medical characteristics of the epidemic were already well-known from the situation in Wuhan. The observation of a first case was the sign that the epidemic had reached the country. We measure the speed of reaction by the delay between this first case and a significant reaction identified when the severity index was greater than 20. We keep in mind that a policy based on herd immunity leads to a late and strong reaction, while a policy based on ICU capacity leads to a much quicker reaction. The delay varies a lot between countries, the maximum being found in the United Kingdom and in Sweden. Smaller countries, except Sweden, reacted in general more quickly. The corresponding level of cases that motivates a sanitary reaction also varies a lot. The value of this number can explain the large number of deaths in the United Kingdom and in Spain. But note the long delay in Germany with the initial small number of cases.

21

Table 6: Policy speed of reaction to the first epidemic outbreak.

Country	First Case	Reaction delay	Cases
United Kingdom	February 1	45	3047
Spain	February 1	37	1527
Italy	January 31	21	3
Germany	January 28	32	57
France	January 25	35	57
Country	First Case	Reaction delay	Cases
Sweden	February 1	46	1063
Belgium	February 4	38	1024
Netherlands	February 28	13	503
Ireland	March 3	11	43
Denmark	February 27	5	5

Note: First Case indicates the date of appearance of the first reported case. Delay is the number of days between the appearance of first cases and a first significant sanitary reaction measured as when the severity index is greater or equal to 20. Cases is the number of cases at the time of sanitary reaction.
Source: University of Oxford, Blavatnik School of Government.

All countries soften their most severe confinement in May for large countries and in June for smaller ones. Table 7 shows that many countries adopted a quick deconfinement with important steps and sometimes re-strengthening their sanitary measures, resulting in some kind of yo-yo policy.

Table 7: Confinement policies and afterward hesitations for deconfinement.

Country	Start	Length	Strength	Changes
United Kingdom	March 24	48	79.6	8 (4)
Spain	March 30	35	85.2	9 (4)
Italy	March 20	21	91.7	6 (7)
Germany	March 22	42	76.9	9 (4)
France	March 17	55	88.0	7 (3)
Country	Start	Length	Strength	Changes
Sweden	April 4	70	46.3	2 (0)
Belgium	March 2	46	81.5	7 (3)
Netherlands	March 31	41	79.6	5 (1)
Ireland	April 6	42	90.7	4 (2)
Denmark	March 18	28	72.2	6 (1)

Note: The column Start indicates the date where the index reaches its first maximum and the column Length corresponds to the length of the period strongest measures. Its level is indicated in the column Strength. The column Changes indicates the number of smoothing changes (*i.e.*, when the value of the index decreases compared to the previous day) after the end of strongest measures till September 28. Between parentheses are indicated the number of restrengthening changes (*i.e.*, when the value of the index increases compared to the previous day).
Source: Authors' own calculations and University of Oxford, Blavatnik School of Government.

There is a contrast between large and small countries, the former having in general shorter strong confinements (except France) followed y a large number of positive and negative adjustments, the latter having longer periods of stronger measures (except Denmark) followed by a small number of adjustments (except Belgium). The case of Sweden is very specific as it adopted no strict confinement *stricto sensus*, but its period of strongest measures is very long, followed by a very small number of adjustments. By early June, most of the small countries had adopted sanitary measures which were softer than those maintained in Sweden. The success of a sanitary policy depends on how a country gets out of its period of confinement. But it also depends on the initial conditions of the epidemic, that is on $\mathcal{R}_0$. So $\mathcal{R}_0$ is very useful for comparing the two waves.

4.4 Estimating the reproduction number for the first wave

Cori et al. (2013) have noted that the expectation of the number of infected people at t is $\mathrm{E}(I_t) = \mathcal{R}_t \sum_s I_{t-s}\omega(s)$ where $\omega(s)$ is the infection profile and $\mathcal{R}_t$ the effective reproduction number. They deduce a general formulation for estimating the effective reproduction number:

$$\mathcal{R}_t = \frac{I_t}{\sum_{s=1}^{t} I_{t-s}\omega(s)},$$

which corresponds to the number of infected at t divided by the number of past infected weighted by their infection profile. However, with COVID-19, the time of infection is not observed, only symptoms are observed, as during the period of incubation there are no symptoms. So $\omega(s)$ is approximated by the serial interval distribution which has to be estimated using individual pairs as reported in section 4.2. Because $\mathcal{R}_t$ estimated in this way is subject to strong variability, Cori et al. (2013) propose to truncate the summation and to use a constant window size h (counted in number of days) such that:[10]

$$\mathcal{R}_t = \frac{I_t}{\sum_{s=1}^{h} I_{t-s}\omega(s)}. \tag{17}$$

The serial interval distribution found in Li et al. (2020) leads to a gamma density with shape parameter of 4.87 and scale parameter of 1.54. With $h = 18$, we have 0.99 of the probability that gamma density.

The major difficulty with formula (17) is that we do not know which value of $\mathcal{R}_t$ to pick because at the beginning of the estimation period $\mathcal{R}_t$ is subject to a strong variability with very high values. We propose to model the epidemic outbreak and to replace I_t in (17) by its predicted value.

---

[10]This formula is implemented in the package `EpiEstim` of R, see Cori et al. (2013).

The usual exponential model is very convenient for this purpose.[11] The exponential model assumes that:

$$\frac{d\,C}{d\,t} = rC(t), \text{ with general solution } C(t) = C_0 \exp(r\,t). \qquad (18)$$

The growth rate per unit of time is r, t is the time index, C_0 is the estimated initial condition. The doubling time, defined as the number of days necessary to double the number of cases, is constant with $\log(2)/r$. Using this model, we replace I_t in (17) by $C'(t)$ so as to get:

$$\mathcal{R}_t = \frac{e^{r\,t}}{\sum_{s=1}^{h} e^{r\,(t-s)}\omega(s)}. \qquad (19)$$

This quantity $\mathcal{R}_t$ is constant over t because of the constant doubling time and converges over h to a finite value, depending on the specification of $\omega(s)$. We take it as a proxy for $\mathcal{R}_0$. A standard deviation can be computed by simulation. Assuming that the distribution of r is a normal density indexed on the classical estimates of this parameter, then for m draws of r, we compute m values of $\mathcal{R}_0$ and then provide the mean and standard deviation of these draws. This is an alternative to bootstrap.

We first estimate the parameters of the exponential model using the confirmed cases data. For each country, the sample starts at the first positive observation and ends at the time of the first serious policy intervention. The latter is determined when the severity index is greater than or equal to 70 (a value usually lower than the maximum of the index) plus 7 days. This corresponds to dates between March 11 and April 3. As for Sweden, the index is always lower than 70, the ending date will be taken when the maximum level of the stringency index is reached, plus 7 days. In Table 8, we present the results for the exponential model and the corresponding $\mathcal{R}_0$ with its associated standard deviation.

The expansion speed of the epidemic is lower for smaller countries, except for Belgium and the Netherlands. The lowest values of $\mathcal{R}_0$ are for Sweden, Denmark, Ireland and Germany. The highest are for Italy and Spain. It seems that Sweden was able to adopt soft confinement measures because its outbreak had a really low speed, resulting in one of the smallest $\mathcal{R}_0$ with Denmark.

4.5 A second wave with different features

After mid-May for large countries and mid-June for smaller countries, European countries started to soften their sanitary policies as detailed in Table 7.

---

[11]The generalized exponential due to Tolle (2003) was used in Viboud et al. (2016) to model epidemic outbreak of various diseases. But this solution is not at adapted as it does not solve the question of choosing which $\mathcal{R}_t$ as the doubling time is not constant in this model.

Table 8: Estimated basic reproduction numbers at the outbreak of the epidemic using the exponential model.

Country	End of outbreak	r	$\mathcal{R}_0$
United Kingdom	Mar 30	0.152	2.79 (0.040)
Spain	Mar 24	0.189	3.46 (0.076)
Italy	Mar 11	0.204	3.79 (0.080)
Germany	Mar 29	0.152	2.79 (0.055)
France	Mar 24	0.167	3.06 (0.050)
Country	End of outbreak	r	$\mathcal{R}_0$
Sweden	Apr 11	0.084	1.81 (0.019)
Belgium	Mar 25	0.176	3.22 (0.066)
Netherlands	Mar 26	0.167	3.05 (0.062)
Ireland	Apr 03	0.131	2.46 (0.078)
Denmark	Mar 25	0.108	2.12 (0.129)

Note: The beginning of the sample is indicated in Table 6 and corresponds to the first observed case. The end of the sample is indicated in column End of outbreak, which corresponds to the date when the stringency index reaches 70 (or its maximum for Sweden) plus 7 days. The growth rate per unit of time is reported in column r. $\mathcal{R}_0$ is computed assuming a Gamma distribution with mean 7.4 and standard deviation 3.4 for the serial interval. Standard deviations are given between parenthesis.
Source: Authors' calculations from data of the University of Oxford, Blavatnik School of Government. Data set retrieved January 26, 2021.

We empirically determine the starting point of a second wave after the end of the strongest confinement period by smoothing out the reported number of new cases and determining the time when it reaches its minimum.[12] We then estimated an exponential model starting from this date and ending the sample when the smoothed severity index starts to climb again after September 20.

The exponential model is fitting quite well, showing that the period does correspond to a new outbreak for cases (see Figure 10). At least two differences with the first wave can be noted from the results in Table 9. The first wave expanded over an average period of two months with a large $\mathcal{R}_0$ (between 1.81 and 3.79). On the contrary, the second wave lasted on average three months, but with an expansion rate which was roughly four times smaller. The estimated $\mathcal{R}_0$ is greater than 1.0, but always lower than 1.37. These differences do not preclude a large expansion of the epidemic as we are nevertheless in an exponential growth.

It is important to stop the sample around this date. After the outbreak of the second wave, data are made difficult to compare. During the first wave, there was a large under-reporting of cases due to the lack of availability for tests (see, *e.g.*, Wu et al. 2020). This was no longer the case for the second

---

[12]We have used the `loess` function of `R` with a smoothing parameter equal to 0.20 and then determined the date of the minimum between June 1 and August 30.

Table 9: Estimated basic reproduction number for a second wave after confinement.

Country	Start	Delay	r	$\mathcal{R}_0$	End
United Kingdom	Jul 09	59	0.043	1.37 (0.005)	Oct 06
Spain	Jun 14	41	0.041	1.35 (0.007)	Sep 21
Italy	Jul 12	69	0.042	1.36 (0.008)	Sep 27
Germany	Jun 06	34	0.025	1.21 (0.003)	Sep 26
France	Jun 18	38	0.041	1.36 (0.005)	Oct 10
Country	Start	Delay	r	$\mathcal{R}_0$	End
Sweden	Jul 23	40	0.027	1.23 (0.004)	Oct 25
Belgium	Jul 03	59	0.033	1.28 (0.005)	Oct 07
Netherlands	Jul 05	55	0.041	1.35 (0.008)	Sep 21
Ireland	Jun 24	37	0.040	1.34 (0.003)	Oct 06
Denmark	Jul 08	84	0.032	1.27 (0.008)	Oct 27

Note: Start indicates the assumed start of the second wave, and Delay the time between the end of the stringiest policy and the empirically determined start of the new wave. End indicates the end of the sample determined as the point where the smoothed severity index starts to increase after September 20. The column r gives the growth rate per unit of time. The reproduction number $\mathcal{R}_0$ is computed assuming a Gamma distribution with mean 7.4 and standard deviation 3.4 for the serial interval. Standard deviations are given between parenthesis.
Source: Authors' calculations from data of the University of Oxford, Blavatnik School of Government. Data set retrieved January 26, 2021.

Figure 10: Outbreak of the second wave
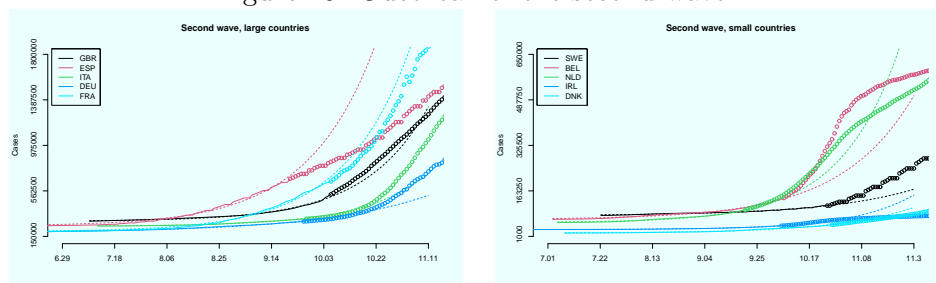
Note: The solid lines represent the observed series used for inference, the dash lines correspond to the prediction of the exponential model. Circle correspond to observed data after the estimation period.

wave. The outbreak of the second wave led to an intensified use of tests and as a consequence more cases were detected.

5 Appraising unconventional sanitary policies

Two cases were amply discussed in the press about the choice they made for containing the epidemic: Sweden and the Netherlands. To summarize, Sweden has relied on voluntary social distancing, but also limiting people gathering and the activity in bars and restaurants. This explains why the

highest value of the Oxford severity index was only 46.30. But the government said also that fighting against the pandemic was a marathon and not a sprint, which explains why the Swedish severity index kept its highest value for so long (70 days) and has decreased only very smoothly. This policy should have caused the peak of the first wave to be reached much earlier, but at the cost of the highest number of deaths compared to the other Nordic countries. The aim was to reach herd immunity as soon as possible. This policy was condemned by its neighbours, Norway, Denmark and Finland which excluded Swedish tourists when reopening their borders.

The Netherlands have also promoted herd immunity in order to implement a targeted lock-down, closing only activities that required close touching, but also closing schools and universities. There was no tight lock-down, people were advised to stay at home, but could go out, provided they respected social distancing. In its implementation, this policy led to a higher but still in a way mild severity index of 79.63, however coupled with a shorter length of 41 days. Here again, this strategy was not appreciated by the neighbouring countries of the Netherlands.

It is however hard to recover these claimed options from Sweden and Netherlands in the Oxford severity index. Sweden reacted very lately (see Table 6), but the Netherland quite quickly which is at odds with a policy based on herd immunity. We must note however that they did not face at all the same $\mathcal{R}_0$ (1.81 versus 3.05). Those data have to be analysed with the help of statistical inference.

5.1 Modelling the first wave and predicting the second wave

With an unconventional policy based on herd immunity, a country should reach the epidemic peak earlier than the other countries and the number of deaths normalized by the population size should be comparable. We have estimated a double Richards and a double Gompertz model for Sweden and the Netherlands on a sample starting on January 22 and ending October 20. As a point of comparison, we have added another Nordic country, Denmark which led a totally conventional policy, based on an early confinement, in accordance with the ICU capacity policy.

We must now comment on the chosen date for the end of our sample. We have collected in Table 10 the reaction dates of all the countries in our sample.

These dates are endogenous as they were motivated by the evolution of the epidemics. If we stop the sample at the first date, we are certainly going to skip the part of the sample which is needed to compare the first wave to the appearance of the second wave. The common date of October 20 corresponds to somewhere between the average date of the first reaction and the average date of the strong reaction. With this choice, the second wave is not fully observed meaning that we have to set an upper limit for

27

Table 10: Policy reactions to the second wave

Country	First Inc.	Strong react	Country	First Inc.	Strong react
UK	Oct 02	Oct 21	Sweden	Oct 22	Dec 03
Spain	Sep 21	Oct 19	Belgium	Oct 11	Nov 15
Italy	Sep 29	Oct 30	Netherlands	Sep 21	Dec 12
Germany	Sep 26	Nov 25	Ireland	Oct 05	Oct 19
France	Oct 06	Nov 01	Denmark	Oct 26	Jan 13
Average	Sep 28	Oct 25	Average	Oct 11	Nov 30

The first date correspond to the date when the smoothed severity index started to increase after September 20. The second date indicate when the smoothed severity index started to be greater than 65.

τ_2. We set a value corresponding to the date of November 10, which could correspond to an assumed date for the peak of the second wave. Using the estimated model, we made predictions till December 31. Results are given in Table 11.

Table 11: Estimated parameters for Cases

	K_i	r_i	δ	Rel Eff	Acc	Peak	Dec
Swe 1	87	0.034	0.65		Apr 23	May 29	Jul 03
Swe 2	183	0.048	0.65	0.48	Oct 17	Nov 12	Dec 06
Nld 1	29	0.103	1.65		Apr 02	Apr 17	May 05
Nld 2	485	0.081	1.65	0.06	Oct 20	Nov 10	Nov 29
Dnk 1	21	0.050	0.14		Mar 19	Apr 10	Apr 30
Dnk 2	176	0.019	0.14	0.12	Sep 16	Nov 09	Dec 31

For each country, the first line corresponds to the parameters for the first wave and the second line for the second wave. K indicates the relative size of the epidemic, r the speed of propagation and δ was imposed to be common to the two waves. The three remarkable moments of each wave are indicated in the last columns.

The best model (according to a BIC) is a Double Richards for all countries.[13] Cases are made comparable, because the data are normalized by population. The most important estimated second wave appears in the Netherlands so that this country gets the worse value for the efficiency index $K1/K2$. Sweden was the last to reach the first peak, at odds with the aim of a herd immunity policy. This peak is also the most important of the three countries. But at the same time, Sweden managed to contain the second peak which occurs around the same date for the three countries and thus it gets the best efficiency index of 0.48. Finally, the total size of the epidemic is very similar in Denmark and in Sweden. It is interesting to note the differences in speed between the two waves. The highest speed during

---

[13]We must note however that the selection between Gompertz and Richards is quite sensitive to the version of the data set and its revision. We used a data set collected on January 26, 2021.

the first wave is reached by the Netherlands, and Denmark has the smallest one for the second wave. The speed decreases in the second wave, except for Sweden where it increases, which denotes a final lack of control for cases in that country as seen from Figure 11 where predictions of cumulative cases are confronted to observed data.
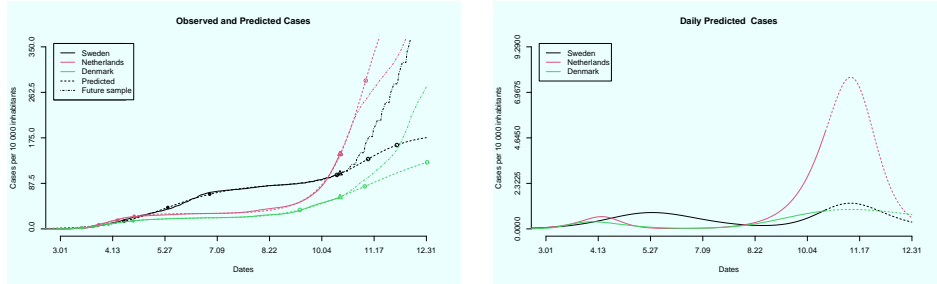

Figure 11: Observed and predicted cumulated and daily cases

In Figure 11 we see that a second wave is predicted from the extrapolation of the sample and that this second wave is more important for the Netherlands.

5.2 Efficiency and the number of deaths

As the final aim is to limit the number of deaths, let us now model it, normalized by population. The optimal model is now the double Gompertz for all countries as indicated in Table 12.

Table 12: Estimated parameters for Deaths

	K_i	r_i	Rel Eff	Acc	Peak	Dec
Swe 1	5.8	0.038		Apr 01	Apr 27	May 22
Swe 2	6.2	0.009	0.93	Oct 20	Oct 21	Oct 21
Nld 1	3.6	0.066		Mar 25	Apr 10	Apr 24
Nld 2	5.3	0.021	0.68	Oct 26	Nov 12	Dec 26
Dnk 1	1.0	0.062		Mar 25	Apr 10	Apr 25
Dnk 2	1.5	0.013	0.69	Sep 02	Nov 02	Dec 31

The first peaks appeared at similar dates for Netherlands and Denmark, a bit later for Sweden. For the second peak, it is not possible to determine a date for Sweden, Netherlands is ten days after Denmark. The relative efficiency is maximum for Sweden and quite large for Netherlands and Denmark. But in term of total size of the epidemic, Denmark has the smallest number of deaths. This last observation might strongly validate its sanitary policy.
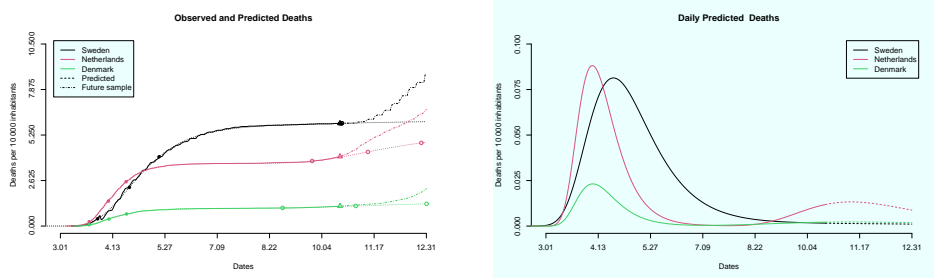
29

Figure 12: Observed and predicted cumulated and daily cases

Figure 12 shows that there is a mild estimated second wave for the Netherland, a tiny one for Denmark and roughly none for Sweden. Because Denmark combines both a very small predicted second wave and the smallest number of death, we can conclude that this country had the best sanitary policy.

If we had extended our sample till December 31 and modified the prior information for the upper limit of τ_2 to November 30, the relative efficiency ranking would not be changed with 0.67 for Sweden, 0.42 for the Netherlands and 0.46 for Denmark. Despite the fact that a large second wave appears in the data after October 20 as shown in Figure 12.

5.3 Comparing the situation in large countries

We do not find any clear-cut policy within the group of large countries, but many hesitations as documented in Table 7. However, Table 10 shows that large countries reacted much earlier to the second wave, a fortnight in advance for the first measures and more than one month for the strongest reactions on average.

Using the same prior and the same sample size, the best model for cases was a double Richards for the UK and a double Gompertz for the remaining countries.

Three countries have a trajectory similar to the Netherlands, even if their policy was largely different: the UK, Spain and France. According to our estimated model and efficiency index, France is an exemplary case of a completely failed deconfinement. Its first wave is smaller and occurred earlier than that of the UK, but its second wave is comparable to that of the UK. So what it has gained during the first wave was lost at the occasion of the second wave. The predicted second wave of Italy and Germany are much smaller, but observed data after October 20 contradict these predictions.

For deaths, there is a more important homogeneity within large countries. A double Gompertz is best all the time. We predict a significant second wave only for Spain as seen in Figure 14, leading to the worse efficient index. On average, large countries reached a greater efficiency for

Table 13: Estimated parameters for Cases, large countries

	K_i	r_i	δ	Rel Eff	Acc	Peak	Dec
UK 1	46	0.049	0.40		Mar 29	Apr 22	May 15
UK 2	362	0.036	0.40	0.12	Oct 10	Nov 12	Dec 13
Spain 1	52	0.076	-		Mar 18	Apr 01	Apr 13
Spain 2	370	0.020	-	0.14	Aug 16	Oct 04	Nov 21
Italy 1	41	0.055	-		Mar 11	Mar 30	Apr 16
Italy 2	151	0.018	-	0.27	Sep 18	Nov 10	Dec 31
Germany 1	23	0.069	-		Mar 17	Apr 01	Apr 14
Germany 2	95	0.012	-	0.24	Aug 24	Oct 29	Dec 31
France 1	30	0.069	-		Mar 23	Apr 07	Apr 21
France 2	469	0.017	-	0.06	Oct 15	Nov 08	Dec 31

For each country, the first line corresponds to the parameters for the first wave and the second line for the second wave. K_i indicates the relative size of the epidemic, r_i the speed of propagation and δ was imposed to be common to the two waves. The three remarkable moments of each wave are indicated in the last columns.
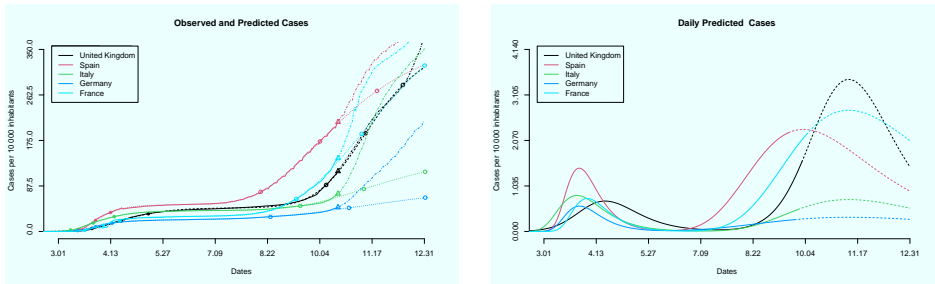

Figure 13: Predicting cases for large European countries

managing the second wave for deaths, slightly better than the Netherlands and Denmark.

Our sample with a fixed end date led to nice predictions for deaths on average. However, Spain has bad predictions and a second wave more important than the others as its second wave started earlier. The left panel of Figure 14 shows that for all countries the observed data after October 20 are much larger than the prediction as if it was not a second wave that was starting, but a second epidemics with a different virus.

6 Discussion and conclusion

The United Kingdom sanitary policy was decided after publishing the dreadful prediction from a SIR-like model where no confinement policy has been introduced. A counterfactual model explores what would happen if a lockdown were implemented. A statistical model does a different job. It is adjusted on observed epidemic data which combines the evolution of the

Table 14: Estimated parameters for Deaths, large countries

	K_i	r_i	Rel Eff	Acc	Peak	Dec
UK 1	6.1	0.060		Mar 30	Apr 16	May 02
UK 2	7.5	0.008	0.81	Oct 07	Nov 04	Dec 31
Spain 1	6.0	0.075		Mar 21	Apr 04	Apr 16
Spain 2	11.2	0.016	0.53	Sep 11	Nov 07	Dec 31
Italy 1	5.7	0.057		Mar 15	Apr 02	Apr 19
Italy 2	6.5	0.008	0.88	Sep 02	Nov 02	Dec 31
Germany 1	1.1	0.070		Mar 30	Apr 14	Apr 27
Germany 2	1.4	0.007	0.74	Aug 20	Oct 27	Dec 31
France 1	4.4	0.078		Mar 27	Apr 09	Apr 21
France 2	6.2	0.011	0.71	Aug 20	Oct 26	Dec 31

For each country, the first line corresponds to the parameters for the first wave and the second line for the second wave. K_i indicates the relative size of the epidemic, r_i the speed of propagation and δ was imposed to be common to the two waves. The three remarkable moments of each wave are indicated in the last columns.
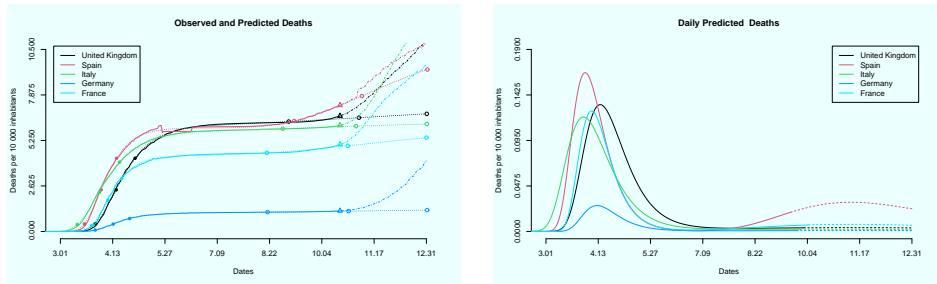

Figure 14: Predicting death for large European countries

epidemic and the effects of the lock-down policy which is applied. A counterfactual exercise is then to show what would have happened if no confinement had been implemented. The role of statistical models is thus quite different from that of compartment models.

A policy is optimal in the SIR model when it manages to reach directly herd immunity. In this context, the policy should led the epidemic develop to reach the optimal rate of contamination and then stop strongly once this rate is reached. This policy is dangerous to implement and possibly feasible only in the case of a very low $\mathcal{R}_0$. Otherwise the number of cases is too important and the public health system will be be overloaded. An alternative policy is to take into account hospital capacity and limit the number of cases to this capacity by an active lockdown. This type of lockdown is totally different with a much earlier reaction. We have identified in some countries these two types of policies, using the Oxford severity index.

We have used statistical models to detect if the epidemic was out of control and in which countries. Essentially these models were estimated to

measure first the speed of propagation of the epidemic at its outbreak and second for comparing the importance of the first and second waves for cases and deaths. This comparison was made difficult because the data have not the same content during the first wave when no or little tests were available and during the second wave when tests were practiced intensively. Inference with those models led us to conclude that the apparent success of a herd immunity policy in Sweden was made possible only because of a very low $\mathcal{R}_0$ compared to other countries during the first wave. The Netherlands that have tried to follow the same route were hampered by a quite higher $\mathcal{R}_0$ so that the epidemic became soon out of control in that country. The success of Sweden has also to be minimized by the high number of deaths that it implied during the first wave. With an early reaction, Denmark was much more successful as it managed to control the epidemic in both waves and to limit drastically the number of deaths. So trying to get herd immunity is not a valid policy objective in the long term. Larger countries were found to be much less efficient in mastering the epidemic on average for cases. But they were quite successful to limit the number of deaths.

A stringent sanitary policy is not easy to implement from a political point of view. Large European countries had many difficulties in defining or just following a coherent policy. The decision for strong confinement was taken everywhere however with differences in the speed of reaction. And everywhere the end of confinement was very erratic. This period was characterized by hesitations, temporary short strengthening followed by small releases. There was a high price to pay for these hesitations, not in the number of deaths, but in the number of cases, at least till October 20. The political cost can be huge if a soft or late policy was chosen at the beginning like in the United Kingdom or in the Netherlands as a much stricter policy had to be introduced later which could lead to strong rejections by the population.

We have used a variety of statistical models, adapted for each case. The exponential model was particularly useful for epidemic outbreaks, before any policy impact, to measure the $\mathcal{R}_0$. The generalized exponential model of Viboud et al. (2016), even if it is very convenient to describe epidemic outbreaks, could not be used as it did lead to any convenient and unique expression for the $\mathcal{R}_0$. Among the various growth models at hand, Gompertz and Richards were particularly useful because of their parsimony and because their are relatively easy to adjust to the data. Double sigmoid models were needed to formalize the possible appearance of a second wave, but can however reach their limits if the data present too many waves. All these models were essential to contrast the characteristics of the epidemic among the ten European countries we have studied.

In this paper, we have treated countries as if their were independent because sanitary policies are defined at the national level (or regional level for Germany). One item of a lock-down policy is to close borders because viruses

circulate over borders. So the interaction between countries (or provinces for China) can be an important factor when modelling the spreading of an epidemic. Cacciapaglia and Sannino (2020) model the log of the cumulative number of infected cases using a simple differential equation which would lead to logistic-like curve in the absence of a supplementary term taking into account neighbouring countries. This is a nice way to appraise the relative efficiency of border control versus social distancing. Hafner (2020) has the same type of concern in a statistical framework using a spatial autoregressive model.

References

Acemoglu, D., Chernozhukov, V., Werning, I., and Whinston, M. D. (2020). Optimal targeted lockdowns in a multi-group SIR model. Discussion paper, MIT Economic Department.

Adam, D. (2020). Special report: The simulations driving the world's response to COVID-19. *Nature*, 580:316–318.

Begley, S. (2020). Influential Covid-19 model uses flawed methods and shouldn't guide U.S. policies, critics say. *Statnews*.

Bock, R. D., Wainer, H., Petersen, A., Thissen, D., Murray, J., and Roche, A. (1973). A parameterization for individual human growth curves. *Human Biology*, 45(1):63–80.

Brent, R. P. (1973). An algorithm with guaranteed convergence for finding a zero of a function. In *Algorithms for Minimization without Derivatives*, chapter 4. Prentice-Hall, Englewood Cliffs, NJ.

Cacciapaglia, G. and Sannino, F. (2020). Interplay of social distancing and border restrictions for pandemics (COVID-19) via the epidemic Renormalisation Group framework. *arXiv*, (2005.04956v1).

Chin, V., Samia, N. I., Marchant, R., Rosen, O., Ioannidis, J. P. A., Tanner, M. A., and Cripps, S. (2020). A case study in model failure? COVID-19 daily deaths and ICU bed utilisation predictions in New York state. *European Journal of Epidemiology*, 35:733–742.

Clancy, D. and O'Neill, P. D. (2008). Bayesian estimation of the basic reproduction number in stochastic epidemic models. *Bayesian Analysis*, 3(4):737–757.

Cori, A., Ferguson, N. M., Fraser, C., and Cauchemez, S. (2013). A new framework and software to estimate time-varying reproduction numbers during epidemics. *American Journal of Epidemiology*, 178(9):1505–1512.

Ferguson, N. M., Laydon, D., Nedjati-Gilani, G., Imai, N., Ainslie, K., Baguelin, M., Bhatia, S., Boonyasiri, A., Cucunuba, Z., Cuomo-Dannenburg, G., Dighe, A., Dorigatti, I., Fu, H., Gaythorpe, K., Green, W., Hamlet, A., Hinsley, W., Okell, L. C., van Elsland, S., Thompson, H., Verity, R., Volz, E., Wang, H., Wang, Y., Walker, P. G., Walters, C., Winskill, P., Whittaker, C., Donnelly, C. A., Riley, S., and Ghani, A. C. (2020). Impact of non-pharmaceutical interventions (NPIs) to reduce COVID-19 mortality and healthcare demand. Report 9, Imperial College.

Gompertz, B. (1825). On the nature of the function expressive of the law of human mortality, and on a new mode of determining the value of life contingencies. *Philosophical Transactions of the Royal Society of London*, 115:513–583.

Hafner, C. (2020). The spread of the Covid-19 pandemic in time and space. *International Journal of Environmental Research and Public Health*, 17(11):3827.

Hale, T., Webster, S., Petherick, A., Phillips, T., and Kira, B. (2020). Oxford COVID-19 Government Response Tracker. Technical report, Blavatnik School of Government, University of Oxford.

Jewell, N. P., Lewnard, J. A., and Jewell, B. L. (2020). Caution warranted: Using the Institute for Health Metrics and Evaluation model for predicting the course of the COVID-19 pandemic. *Annals of Internal Medicine*, 173(3):226–227.

Kermack, W. O. and McKendrick, A. G. (1927). A contribution to the mathematical theory of epidemics. *Proceedings of the Royal Society A*, 115(772):700–721.

Li, Q., Guan, X., Wu, P., Wang, X., Zhou, L., Tong, Y., Ren, R., Leung, K. S., Lau, E. H., Wong, J. Y., Xing, X., Xiang, N., Wu, Y., Li, C., Chen, Q., Li, D., Liu, T., Zhao, J., Liu, M., Tu, W., Chen, C., Jin, L., Yang, R., Wang, Q., Zhou, S., Wang, R., Liu, H., Luo, Y., Liu, Y., Shao, G., Li, H., Tao, Z., Yang, Y., Deng, Z., Liu, B., Ma, Z., Zhang, Y., Shi, G., Lam, T. T., Wu, J. T., Gao, G. F., Cowling, B. J., Yang, B., Leung, G. M., and Feng, Z. (2020). Early transmission dynamics in Wuhan, China, of novel coronavirus-infected pneumonia. *New England Journal of Medicine*, 382(13):1199–1207.

Lipovetsky, S. (2010). Double logistic curve in regression modeling. *Journal of Applied Statistics*, 37(11):1785–1793.

Ma, J. (2020). Estimating epidemic exponential growth rate and basic reproduction number. *Infectious Disease Modelling*, 5:129–141.

Moll, B. (2020). Lockdowns in SIR models. Technical report, LSE.

Oswald, S. A., Nisbet, I. C. T., Chiaradia, A., and Arnold, J. M. (2012). FlexParamCurve: R package for flexible fitting of nonlinear parametric curves. *Methods in Ecology and Evolution*, 3(6):1073–1077.

Park, M., Cook, A. R., Lim, J. T., Sun, Y., and Dickens, B. L. (2020). A Systematic Review of COVID-19 Epidemiology Based on Current Evidence. *Journal of Clinical Medicine*, 9(4). 967.

Pathak, A., Mohan, V. M., and Banerjee, A. (2020). Optimal lockdown strategies for SARS-CoV2 mitigation: an Indian perspective. *medRxiv*, pages 1–20.

Rachel, L. (2020). An analytical model of Covid-19 lockdowns. Technical report, London School of Economics.

Richards, F. J. (1959). A flexible growth function for empirical use. *Journal of Experimental Botany*, 10(2):290–301.

Roques, L., Klein, E., Papax, J., Sar, A., and Soubeyrand, S. (2020). Using early data to estimate the actual infection fatality ratio from COVID-19 in France. *MDPI Biology*, 9(5):1–12.

Thissen, D., Bock, R. D., Wainer, H., and Roche, A. F. (1976). Individual growth in stature: A comparison of four growth studies in the U.S.A. *Annals of Human Biology*, 3(6):529–542.

Toda, A. A. (2020). Susceptible-infected-recovered (SIR) dynamics of COVID-19 and economic impact. Technical report, arXiv:2003.11221v2.

Tolle, J. (2003). 87.65 can growth be faster than exponential, and just how slow is the logarithm? *The Mathematical Gazette*, 87(510):522–525.

Tsoularis, A. and Wallace, J. (2002). Analysis of logistic growth models. *Mathematical Biosciences*, 179(1):21–55.

Turner, M. E., Bradley, E. L., Kirk, K. A., and Pruitt, K. M. (1976). A theory of growth. *Mathematical Biosciences*, 29(3):367 – 373.

Verhulst, P. F. (1845). Recherches mathématiques sur la loi d'accroissement de la population. *Nouveaux mémoires de l'Académie Royale des Sciences et Belles-Lettres de Bruxelles*, 18:14–54.

Vespignani, A. (2011). Modelling dynamical processes in complex socio-technical systems. *Nature Physics*, 8(1):32–39.

Viboud, C., Simonsen, L., and Chowell, G. (2016). A generalized-growth model to characterize the early ascending phase of infectious disease outbreaks. *Epidemics*, 15:27 – 37.

Wang, H., Wang, Z., Dong, Y., Chang, R., Xu, C., Yu, X., Zhang, S., Tsamlag, L., Shang, M., Huang, J., et al. (2020). Phase-adjusted estimation of the number of coronavirus disease 2019 cases in Wuhan, China. *Cell discovery*, 6(1):1–8.

Wang, X.-S., Wu, J., and Yang, Y. (2012). Richards model revisited: Validation by and application to infection dynamics. *Journal of Theoretical Biology*, 313:12–19.

Wu, S. L., Mertens, A. N., Crider, Y. S., Nguyen, A., Pokpongkiat, N. N., Djajadi, S., Seth, A., Hsiang, M. S., Colford Jr., J. M., Reingold, A., Arnold, B. F., Hubbard, A., and Benjamin-Chung, J. (2020). Substantial underestimation of SARS-CoV-2 infection in the United States. *Nature Communications*, 11(4507).